Raman spectroscopy and photoluminescence of ZnTe thin films grown on GaAs

J. Camacho[a] and A. Cantarero
Materials Science Institute, University of Valencia, P. O. Box 22085, E-46071 Valencia, Spain

I. Hernández-Calderón
Departamento de Física, CINVESTAV-IPN, Apartado Postal 14740, 07000 Mexico Distrito Federale, Mexico

L. González
Instituto de Microelectrónica de Madrid, CNM-CSIC, E-28760 Tres-Cantos, Madrid, Spain

(Received 8 February 2002; accepted 27 August 2002)

We report resonant Raman scattering and photoluminescence (PL) measurements on two ZnTe thin films grown by molecular-beam epitaxy on GaAs substrates with thicknesses around 0.5 and 1.0 μm. The data have been obtained by using the different excitation energies of an Ar^+ laser to distinguish Raman from PL and analyze resonant effects. The characteristic features of the low-temperature PL spectra are the light and heavy free exciton emissions, split due to the thermal strain effect, followed by several phonon replicas of these lines. Moreover, longitudinal and transversal polariton splittings of heavy excitons are clearly observed. Their reduced masses have been obtained from the exciton binding energies. Room and low-temperature Raman spectra show, besides the typical longitudinal optical (LO) multiphonon emissions, forbidden zone-center transverse optical (TO) + $(n-1)$LO phonon combinations, which yield an accurate value for the LO and TO phonon energies. The breakdown of the selection rules is attributed to surface faceting. [DOI: 10.1063/1.1516267]

I. INTRODUCTION

Zinc telluride and other II–VI semiconductors and their alloys are promising materials in the fabrication of light-emitting devices in the visible and near ultraviolet optical range. In recent years, much work, including Raman scattering,[1–3] has been devoted to the study of the optical properties of ZnTe. Although the electronic and vibrational properties of bulk ZnTe are already well known, some discrepancies concerning the interpretation of the photoluminescence (PL) results have appeared in literature[2,4] most of them arising from the different methods of growth and thermal expansion effects. Zhang *et al.*[2] reported a comparison of the different assignments of the PL features in literature for ZnTe bulk and the epilayers ZnTe/GaAs and ZnTe/GaSb. A more recent work on ZnTe epilayers[5] gives a detailed study of the PL emissions including the dependence on temperature of the band gap as well as the intensity and full width at half maximum of the free exciton peak and acceptor bound excitonic emissions. The effects of biaxial strain in ZnTe/InAs thin films have also been investigated by Raman scattering spectroscopy under pressure[3] obtaining the phonon deformation potentials (PDP). The longitudinal optical (LO) multiphonon emission in bulk ZnTe is analyzed in Ref. 6, where a simple analytical expression explains all the emissions as outgoing resonances.

The growth of ZnTe thin films on GaAs (100) substrates provides us with a direct application of the fabrication of optoelectronic devices. Since both materials have a zinc blende structure, the growth by molecular-beam epitaxy (MBE) is proven to give samples with an excellent crystalline quality (in spite of the lattice mismatch, around 8%). The strain in lattice-mismatched semiconductor systems can be maintained homogeneously and stably as long as the layers are kept sufficiently thin, namely, thinner than the critical thickness (h_c) at which defects are generated. When the layer thickness exceeds the critical thickness, the strain relaxes through the appearance of misfit dislocations. Although ZnTe films are thought to grow unstrained due to the formation of dislocations and/or defects,[7] as the sample is cooled, there exists an induced thermal stress due to the difference in thermal expansion coefficients of ZnTe and GaAs between the growth temperature and the temperature at which the measurements are performed. As a consequence of the strain, not only changes in the lattice parameter are produced, but also the electronic band structure and vibrational modes are affected.

In this work, we present Raman scattering measurements in two ZnTe/GaAs heterostructures, whose thicknesses are well above h_c. Due to the measurement conditions (excitation wavelength above the band-gap energy), the spectra show the Raman peaks superimposed on the luminescence. The energy difference corresponding to the light- (lh) and heavy-hole (hh) excitons splitting agrees with the calculated difference due to thermal strain effects. The binding energy and the reduced masses of the lh and hh excitons are determined. Up to third-order LO-phonon replicas of some exciton PL emissions are observed. Raman spectra at low tem-

[a]Also at: Dpto. Física Aplicada, Universidad Politécnica de Cartagena, E-30202 Murcia, Spain; electronic mail: jcamacho@uv.es

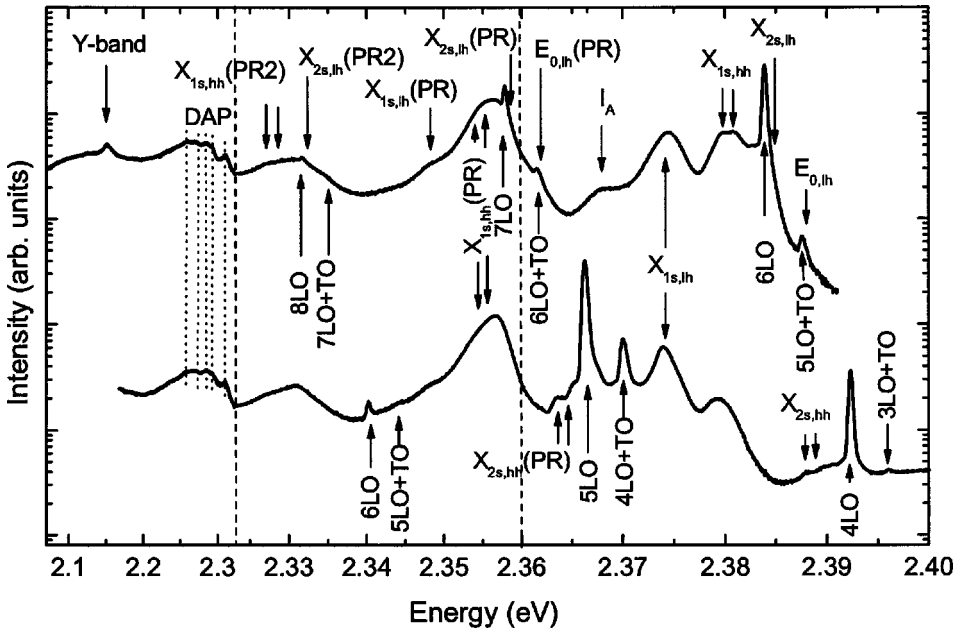

FIG. 1. Photoluminescence of ZnTe/GaAs (sample A) obtained with excitation wavelengths 496.5 nm (gray line) and 486.9 nm (black line) measured at low temperature (19 K). The label of the PL peaks is in agreement with the calculated splitting [Eq. (3)]. The Raman peaks are indicated at the bottom. The figure is separated into three regions, marked by vertical lines, with different scale.

perature show up to the tenth LO-phonon overtones. Moreover, a noticeable fact of the spectra is the appearance of features related to $\mathrm{TO}+(n-1)\mathrm{LO}$ zone-center multiphonon combinations.

II. EXPERIMENTAL DETAILS

The two samples under study are ZnTe thin films grown on GaAs (100) substrates by MBE at a rate of $\sim 0.52\ \mu$m per hour employing solid sources of Zn and Te. The growth was performed under Te-rich conditions. The surface of the samples exhibited a (2×1) reconstruction as it was observed by reflection high-energy electron diffraction. The growth temperatures, as monitored by an optical pyrometer, were 290 °C and 292 °C for samples labeled A and B, respectively. Their thicknesses are 1 μm (sample A) and 0.53 μm (sample B). Raman measurements were performed at room temperature and at 19 K in backscattering configuration. For the low-temperature measurements, a cryostat with a closed-cycle cryocooler system was used. Four different wavelengths of an Ar^+ laser: 514.5 (2.41), 496.5 (2.50), 487.9 (2.54), and 476.5 nm (2.60 eV), were used as excitation source. The laser power was kept below 20 mW. All the PL spectra were obtained in the same conditions. The samples were characterized by x-ray diffraction measurements by means of $\omega/2\theta$ scans at the (004) reflection in the $(\pm)$ Bragg arrangement along $\langle 100\rangle$.

III. EXPERIMENTAL RESULTS AND DISCUSSION

The lattice parameters of samples A ($a_\parallel = 6.106$ Å and $a_\perp = 6.101$ Å) and B ($a_\parallel = 6.105$ Å and $a_\perp = 6.103$ Å) obtained by x-ray diffraction measurements at room temperature show that both samples are practically relaxed ($a_{\mathrm{ZnTe}} = 6.1037$ Å from Ref. 8), as could be expected since the thicknesses of the films under study are much larger than the critical thickness h_c ($h_c = 15$ Å for epitaxial growth of ZnTe on (001) GaAs substrates by MBE).[9]

For the comparison with the experimental results, the in-plane constant $a_\parallel$ at any temperature can be calculated as[1]

$$a_\parallel = a_{\mathrm{ZnTe}}(1+\delta), \tag{1}$$

with

$$\delta = K\int (\alpha_{\mathrm{ZnTe}} - \alpha_{\mathrm{GaAs}})dT + (K-1)\frac{a_{\mathrm{ZnTe}} - a_{\mathrm{GaAs}}}{a_{\mathrm{ZnTe}}}, \tag{2}$$

where a_{ZnTe} and a_{GaAs} are the lattice parameters of bulk ZnTe and GaAs, respectively. K describes the value of the lattice relaxation, $K=0$ for a layer thickness below h_c and $K=1$ for complete relaxation of the misfit strain in thick layers. α_{ZnTe} and α_{GaAs} are the thermal expansion coefficients of ZnTe and GaAs, respectively. Since the thicknesses of our ZnTe/GaAs samples are much larger than h_c, one can set $K=1$ in the present study. Hence, only the first term on the right-hand side of Eq. (2) is considered in the calculation of $a_\parallel$. Due to the temperature dependence of the thermal expansion coefficients of both materials, it is necessary to perform an integral between the growth temperature and that at which PL measurements were carried out (19 K). Data of α_{GaAs} and α_{ZnTe} from Refs. 10 and 11, respectively, were used. The result gives an in-plane tensile strain of 7.07×10^{-4} (7.09×10^{-4}) for sample A (B). Thus, the values of $a_\parallel$ for samples A and B are nearly coincident ($a_\parallel \approx 6.108$ Å).

A. Photoluminescence

The effect of strain on the electronic properties is a splitting of the four-fold degenerate $P_{3/2}$ valence-band maxima at $\mathbf{k}=0$. It has been shown[1] that for layers grown thicker than h_c, the mismatch strain is mainly relaxed by the creation of misfit dislocations, being the hh and lh exciton splitting dominated by the thermal induced strain. Moreover, due to the exciton–polariton coupling, the hh exciton splits into a doublet as can be seen in Fig. 1, where luminescence spectra from sample A obtained with excitation wavelengths 496.5 nm (lower line) and 486.9 nm (upper line) are shown. The

TABLE I. Assignments and energies of the luminescence features of the sample A.

Assignment	Energy (eV)	Description
$X_{2s,hh}$	2.391, 2.390	Excited state free hh exciton (doublet)
$E_{0,lh}$	2.387	lh-exciton continuous
$X_{2s,lh}$	2.384	Excited state free lh exciton
$X_{1s,hh}$	2.381, 2.380	Ground-state free hh exciton (doublet)
$X_{1s,lh}$	2.375	Ground-state free lh exciton
I_A	2.368	Shallow acceptor
$X_{2s,hh}$(PR)	2.365, 2.364	First LO-phonon replica of $X_{2s,hh}$
$X_{2s,lh}$(PR)	2.358	First LO-phonon replica of $X_{2s,lh}$
$X_{1s,hh}$(PR)	2.355, 2.354	First LO-phonon replica of $X_{1s,hh}$
$X_{1s,lh}$(PR)	2.349	First LO-phonon replica of $X_{1s,lh}$
$X_{1s,hh}$(PR2)	2.323	Second LO-phonon replica of $X_{1s,hh}$

assignments of the emission energies are consistent with previous works[2,5] corresponding to thicker epilayers. The descriptions and the corresponding energies of the PL peaks are listed in Table I. The features at higher energy (2.391 and 2.390 eV) correspond to the doublet of the first-excited state of the hh exciton due to exciton–polariton effects (upper and lower polariton branches, $\Delta E_{UL} \sim 1.2$ meV). The first-excited state of the lh exciton is found at 2.384 eV. The splitting is also observed in the case of the ground state of the hh exciton. Regarding the emission from the lh ground-state exciton ($X_{1s,lh}$), the exciton–polariton effect is hidden by a broad peak. The phonon peaks, which appear on top of the luminescence, are labeled in Fig. 1. The features around 2.3 eV are known as the recombination due to the emission of donor–acceptor pairs,[12] and that around 2.15 eV is known as the *Y* band.[5] This latter structure, which usually appears at ~200 meV below the band gap, seems to be related to misfit dislocations. Some phonon replicas (PR) of the exciton energies are also observed in our PL spectra (see Table I).

The shift of the hh and lh band gaps can be calculated in terms of the thermal strain[1]

$$\Delta E = \left(-2a \frac{c_{11}-c_{12}}{c_{11}} \pm b \frac{c_{11}+2c_{12}}{c_{11}} \right) \epsilon. \tag{3}$$

Here, a and b are, respectively, the hydrostatic and shear electron deformation potentials (DPs), c_{ij} are the elastic compliances, whose values are $c_{11}=71.1$ GPa, $c_{12}=40.7$ GPa (Ref. 13), and ϵ is the stress magnitude. The $+(-)$ sign corresponds to $\Delta E_{hh}(\Delta E_{lh})$.

Using the values of the elastic compliances just given, and the DPs of ZnTe, $a=-5.4$ (Ref. 14) and $b=-1.8$,[12] together with the value of $\epsilon \sim 7.1\times10^{-4}$, the calculated $\Delta E_{1s,lh}-\Delta E_{1s,hh}$ splitting is 5.5(1) meV for both samples, which is in overall agreement with the experimental splitting around 5.6 meV. Figure 2 depicts representative excitonic-band structure levels of the samples under study. Only the ground state ($n=1$) and the first-excited state ($n=2$) of the lh (dashed line) and hh (solid line) excitons are plotted together with the continuous band. Exciton–polariton coupling effects have been omitted in Fig. 2 for simplicity. The arrows indicate transition energies from the exciton levels. The free-lh (hh) exciton binding-energy R^* is determined from the $n=1$ and $n=2$ free-exciton emission

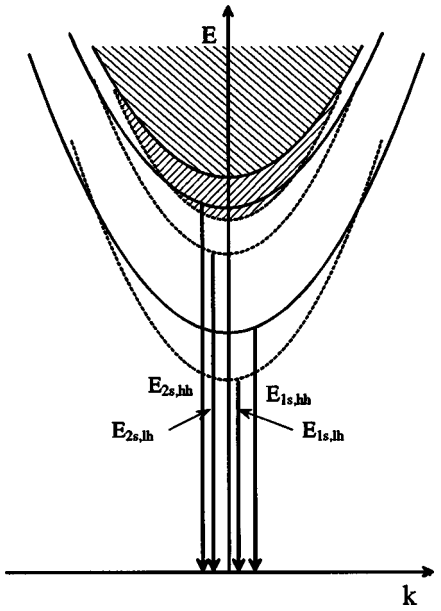

FIG. 2. Band structure excitonic levels of ZnTe/GaAs under tensile biaxial strain. The lh and hh excitons split because of the strain. Exciton–polariton effects are not included for simplicity.

$$E_{1s}-E_{2s}=\frac{3}{4}\frac{\mu R_H}{m_0\epsilon_0^2}=\frac{3}{4}R^*, \tag{4}$$

in eV, where R_H is the Rydberg of the hydrogen atom, μ is the reduced mass of the exciton, m_0 is the free electron mass, and ϵ_0 is the static dielectric constant. The experimental values found for the heavy and light Rydbergs are $R^*_{hh}=12.93$ and $R^*_{lh}=12.53$ meV, respectively. By using $\epsilon_0=9.4$,[15] we find an exciton reduced mass of $0.084m_0$ and $0.081m_0$ for the heavy and light, respectively. The heavy exciton reduced mass coincides with the value given in Ref. 15. From this value for the Rydberg and the splitting between light and heavy excitons, we deduced that the transition $E_{2s,hh}$ is within the light hole exciton continuum and thus it is hardly observable (see Fig. 1).

B. Raman scattering

Figure 3 shows Raman spectra of samples A and B taken at room temperature with the 514.5 nm excitation wavelength. The luminescence (dashed line), with the main peak around 2.259 eV, has been subtracted in order to have a better insight of each contribution. Besides the nLO multiphonon overtones (up to the seventh order is observed at room temperature), TO$+(n-1)$LO zone-center phonon combinations appear below the nLO peaks, whereas tails probably due to phonon density of states are observed at frequencies higher than the nLO multiphonon overtones. The frequency of the different phonon modes (up to $n=7$) are multiples of $\omega_{LO}=205.02\pm0.03$ cm^{-1}, which indicates that mainly $k=0$ electronic states contribute to the resonances. The Raman frequencies in both samples are the same.

Raman spectra of sample B at 19 K with the four excitation wavelengths used are depicted in Fig. 4, where the labels indicate only the Raman peaks; the unlabeled peaks are the luminescence lines already discussed (see Fig. 1).

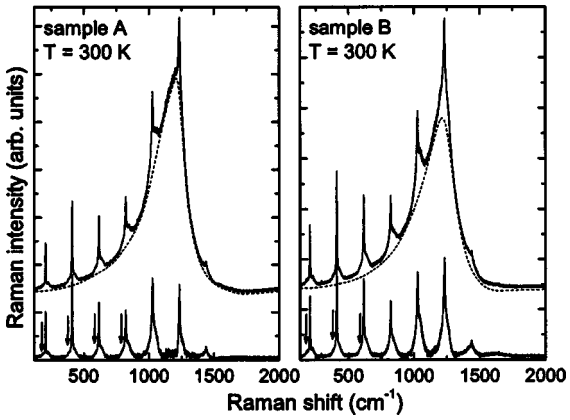

FIG. 3. Raman spectra of both samples at room temperature. The arrows indicate the position of the TO+$(n-1)$LO zone-center phonon combinations. The Raman peaks appear on top of the luminescence, which has been subtracted in the spectra shown at the bottom.

The results obtained with sample A are coincident. The windows shown for each excitation wavelength (λ_{exc}) correspond to the spectral region where Raman peaks are enhanced by resonance effects. The increase in intensity of the multiphonon peaks is due to the matching of the excitation energy to electronic transitions (outgoing resonances). Up to the tenth order of the LO multiphonon emission is observed with the 476.5 nm excitation wavelength. The LO-phonon frequency obtained from the experiment is $\omega_{LO}=210.45\pm0.02\,cm^{-1}$, while the ninth overtone is at $\omega_{2LO}=1894.22\pm0.12$, exactly nine times the value corresponding to the first Raman peak (the other overtones are exactly multiples of the first phonon energy, up to $n=10$), i. e., the value is also accurate. There is a blueshift of $\Delta\omega=5.43\pm0.05\,cm^{-1}$, when compared to high temperature data.

Since our measurements were performed in backscattering geometry and the samples are grown in the (001) direction, the TO mode is forbidden. However, we can clearly see, for some wavelengths, the TO and a series of peaks corresponding to the TO+nLO contributions. We attribute the relaxation of the selection rules to the presence of some faceting on the surface of the samples originated during the growth.[16] From the measurements at room and low temperatures, we obtain $\omega_{TO}=176.5\pm0.8$ and $\omega_{TO}=180.63\pm0.04\,cm^{-1}$, respectively.

The shift of the phonon frequency with stress is given by

$$\frac{\Delta\omega}{\omega_0}=\left[\tilde{K}_{12}-\tilde{K}_{11}\frac{c_{12}}{c_{11}}\right]\epsilon_{xx}, \tag{5}$$

where $\tilde{K}_{11}$ and $\tilde{K}_{12}$ are the PDP (Ref. 17). Using the values of the PDP given in Ref. 3 $\tilde{K}_{11}=-2.3(3)$ and $\tilde{K}_{12}=-1.7(3)$, and the stress obtained from the analysis of the PL data ($\epsilon\approx7.1\times10^{-4}$), $\Delta\omega/\omega_0\simeq2.7\times10^{-4}$. Thus, the measured shift can not be explained by thermal expansion effects. Instead, the main reason of this strong variation of the phonon frequencies with temperature is directly connected to anarmonicity effects.[18]

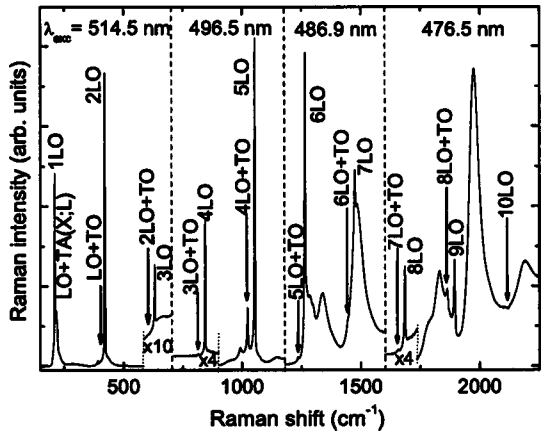

FIG. 4. Raman spectra of ZnTe/GaAs (sample B) at $T=19$ K. The assignment of Raman features to one- and two-phonon combinations is indicated in the figure. The unlabeled peaks correspond to luminescence features (see Fig. 1).

IV. CONCLUSIONS

We have performed Raman scattering measurements in two ZnTe thin films grown on GaAs (001) substrates with thicknesses around 0.5 and 1.0 μm. The assignment of the luminescence peaks is in good agreement with previous works. The binding energy of the lh and hh excitons has been obtained from the experimental data taking into account the thermal strain. The splitting between them has been calculated and it is in full agreement with the experimental value. The lh and hh excitons reduced masses have been determined. From the Raman scattering carried out at room and low temperature, we have observed the presence of TO+$(n-1)$LO zone-center phonon-combinations, which are attributed to surface faceting originated during the growth. Finally, the Raman stokes shift of the LO and TO phonons have been accurately determined. At room temperature, $\omega_{LO}=205.02\pm0.03\,cm^{-1}$ and $\omega_{TO}=176.5\pm0.8$, while at low temperature (19 K), $\omega_{LO}=210.45\pm0.02\,cm^{-1}$ and $\omega_{TO}=180.63\pm0.04\,cm^{-1}$.

ACKNOWLEDGMENTS

One of the authors (A.C.) wishes to acknowledge the Dirección de Relaciones Internacionales of the University of Valencia for financial support. Another author (I.H.C.) thanks CONACyT-Mexico for partial support.

[1] J. Gutowski, Semicond. Sci. Technol. **6**, A51 (1991).
[2] Y. Zhang, B. J. Skromme, and F. S. Turco-Sandroff, Phys. Rev. B **46**, 3872 (1992), and references herein.
[3] R. J. Thomas, M. S. Boley, H. R. Chandrasekhar, M. Chandraekhar, C. Parks, A. K. Ramdas, J. Han, M. Kobayashi, and R. L. Gunshor, Phys. Rev. B **49**, 2181 (1994).
[4] H. Leiderer, G. Jahn, M. Silberbauer, W. Kuhn, H. P. Wagner, W. Limmer, and W. Gebhardt, J. Appl. Phys. **70**, 398 (1991).

[5] Y.-M. Yu, S. Nam, K-S. Lee, Y. D. Choi, and B. O, J. Appl. Phys. **90**, 807 (2001).
[6] Z. C. Feng, S. Perkowitz, and P. Becla, Solid State Commun. **78**, 1011 (1991).
[7] B. A. Wilson, C. E. Bonner, R. D. Feldman, R. F. Austin, D. W. Kisker, J. J. Krajewski, and P. M. Bridenbaugh, J. Appl. Phys. **64**, 3210 (1988).
[8] Landolt-Börnstein, in *Numerical Data and Functional Relationships in Science and Technology*, Tables Vol. 41, edited by U. Rössler (Springer, Berlin, 1999), Subvolume B.
[9] V. H. Etgens, M. Sauvage-Simkin, R. Pinchaux, J. Massies, N. Jedrecy, A. Waldhauer, S. Tatarenko, and P. H. Jouneau, Phys. Rev. B **47**, 10607 (1993).
[10] Y. S. Touloukian, R. K. Kirby, R. E. Taylor, and T. Y. R. Lee, *Thermal Expansion* (IFI/Plenum, New York, 1977), Vol. 13.
[11] J. Camacho, I. Loa, A. Cantarero, and K. Syassen, J. Phys.: Condens. Matter **14**, 739 (2002).
[12] M. Ekawa and T. Taguchi, Jpn. J. Appl. Phys., Part 2 **38**, L1341 (1989).
[13] D. Belincourt, H. Jaffe, and L. R. Shiozawa, Phys. Rev. **129**, 1009 (1963).
[14] K. Strössner, S. Ves, C. K. Kim, and M. Cardona, Solid State Commun. **61**, 275 (1987).
[15] H. P. Wagner, S. Lankes, K. Wolf, D. Lichtenberger, W. Kuhn, P. Link, and W. Gebhardt, J. Lumin. **52**, 41 (1992).
[16] I. Hernández-Calderón *et al.* (unpublished).
[17] E. Anastassakis and M. Cardona in *Phonons, Strains, and Pressure in Semiconductors*, High Pressure in Semiconductor Physics II, Semiconductors and Semimetals Vol. II, (Academic New York, 1996).
[18] J. L. Lacombe and J. C. Irwin, Solid State Commun. **8**, 1427 (1970).